International Journal of Pharmaceutics 597 (2021) 120287

Contents lists available at ScienceDirect

International Journal of Pharmaceutics

journal homepage: www.elsevier.com/locate/ijpharm

Preparation and evaluation of PEG-coated zein nanoparticles for oral drug delivery purposes

C. Reboredo [a], C.J. González-Navarro [b], C. Martínez-Oharriz [c], A.L. Martínez-López [a], J. M. Irache [a,*]

[a] Department of Chemistry and Pharmaceutical Technology, University of Navarra, C/ Irunlarrea 1, 31008 Pamplona, Spain
[b] Centre for Nutrition Research, University of Navarra, C/ Irunlarrea 1, 31008 Pamplona, Spain
[c] Department of Chemistry, University of Navarra, C/ Irunlarrea 1, 31008 Pamplona, Spain

ARTICLE INFO

Keywords:
Nanoparticles
Zein
PEG
Mucus-permeating
Oral delivery

ABSTRACT

The aim was to produce PEG-coated nanoparticles (NP-PEG), with mucus-permeating properties, for oral drug delivery purposes by using simple procedures and regulatory-approved compounds in order to facilitate a potential clinical development. For this purpose, zein nanoparticles were prepared by desolvation and, then, coated by incubation with PEG 35,000. The resulting nanocarriers displayed a mean size of about 200 nm and a negative zeta potential. The presence of PEG on the surface of nanoparticles was evidenced by electron microscopy and confirmed by FTIR analysis. Likely, the hydrophobic surface of zein nanoparticles (NP) was significantly reduce by their coating with PEG. This increase of the hydrophilicity of PEG-coated nanoparticles was associated with an important increase of their mobility in pig intestinal mucus. In laboratory animals, NP-PEG (fluorescently labelled with Lumogen® Red 305) displayed a different behavior when compared with bare nanoparticles. After oral administration, NP appeared to be trapped in the mucus mesh, whereas NP-PEG were capable of crossing the protective mucus layer and reach the epithelium. Finally, PEG-coated zein nanoparticles, prepared by a simple and reproducible method without employing reactive reagents, may be adequate carriers for promoting the oral bioavailability of biomacromolecules and other biologically active compounds with low permeability properties.

1. Introduction

In the last decades, numerous efforts have been performed in order to develop new and effective treatments for a multitude of diseases based on the use of nanodevices (e.g., liposomes, nanoparticles, micelles, dendrimers, etc.) as drug delivery systems. Many of these developments have clearly demonstrated (in preclinical studies) multiple benefits in treating chronic diseases, including important improvements in the therapeutic index of antimicrobials (Pison et al., 2006; Singh and Nalwa, 2011) or anticancer drugs (Gurunathan et al., 2018; Ma and Mumper, 2013). These improvements are directly related to the capabilities of these nanodevices to protect the loaded drug against a premature degradation in the body improving its bioavailability, or/and to increase the therapeutic agent in its site of action (Irache et al., 2011; Vinogradov and Wei, 2012). Nevertheless, the number of these nanoparticles that have reached commercialization after a successful clinical trial is extremely low. At this moment, there would be around 20 commercial nano-based drugs approved by Regulatory Agencies (Bhardwaj et al., 2019), particularly based on the use of liposomes and polymers to encapsulate drugs inside their core and intended for cancer therapy (Hua et al., 2018). In addition, an estimated 100 nanoparticle-based products are in clinical trials, of which 18 started in the past 3 years (Martins et al., 2020); although, only six would be intended for oral administration (ClinicalTrials.gov, 2021).

This relatively low number of "successful" developments is (at least in part) related with a long and challenging regulatory pathway (Bremer-Hoffmann et al., 2018; Gaspani and Milani, 2013); surely influenced by a vague definition of the term "nanoparticle" and a certain negative state of public opinion (Bhardwaj et al., 2019) with everything that the term "nano" means or includes. Other barriers that importantly hamper the clinical development of nanoparticles for drug delivery purposes include the use of "innovative" materials rather than the approved excipients and the difficulties to scale-up and transfer the whole preparative process to an industrial environment. In this way, the formulation of nanoparticles with a compound without a regulatory status (i.e., excipient or GRAS) makes the development process more

* Corresponding author.
E-mail address: jmirache@unav.es (J.M. Irache).

https://doi.org/10.1016/j.ijpharm.2021.120287
Received 28 October 2020; Received in revised form 16 January 2021; Accepted 17 January 2021
Available online 29 January 2021

challenging, longer and, therefore, more expensive (Cicha et al., 2018). This would be the case when nanoparticles are prepared with a new synthetic polymer, where additional information is required to demonstrate its safety with respect to the currently proposed level of exposure or administration route.

Moreover, the employment of toxic reagents or organic solvents for the synthesis of nanoparticles as well as the complexity and reproducibility of the preparative method are also important aspects that will hinder the continuity of the project towards clinical phases. Nevertheless, the robustness of the process has to be evaluated as a whole, including all the steps and procedures involved in the manufacture of the final product (i.e., purification, concentration and drying steps).

In this context, the aim of this work was to produce mucus-permeating nanocarriers for oral drug delivery purposes by using simple procedures and regulatory-approved compounds in order to facilitate a potential clinical development. Mucus-permeating nanocarriers have the capability of minimizing the interaction with the mucus mesh (Netsomboon and Bernkop-Schnürch, 2016) and, thus, promoting diffusing through its protective layer lining the epithelium (Maisel et al., 2016; Netsomboon and Bernkop-Schnürch, 2016). The use of this type of nanocarriers may be of interest to improve the oral bioavailability of biomacromolecules (Ensign et al., 2012) and other biologically active compounds with low permeability properties. For this purpose, zein-based nanoparticles prepared by a desolvation procedure and coated by simple adsorption with poly(ethylene glycol) (PEG) were prepared and evaluated. Zein is the main protein from corn with a hydrophobic character and insoluble in water that possesses a GRAS regulatory status (Irache and González-Navarro, 2017; Penalva et al., 2015). PEGs are hydrophilic neutral polymers approved as excipients and widely employed in several cosmetic and pharmacological products due to its safeness (D'souza and Shegokar, 2016).

2. Materials and methods

2.1. Materials

Zein, lysine, poly(ethylene glycol) 35,000 Da (PEG35), and Rose Bengal sodium salt were purchased from Sigma-Aldrich (Steinheim, Germany). Ethanol absolut was obtained from Scharlab (Sentmenat, Spain). Lumogen® Red 305 was provided by BASF (Ludwigshafen am Rhein, Germany). Mannitol was purchased from Guinama (La Pobla de Vallbona, Spain). O.C.T.™ Compound Tissue-Tek was obtained from Sakura Finetek Europe (Alphen aan Der Rijn, The Netherlands).

2.2. Preparation of nanoparticles

2.2.1. Preparation of bare nanoparticles (NP)

Zein nanoparticles were prepared by a desolvation procedure previously described (Penalva et al., 2015), with minor modifications. Briefly, 200 mg zein and 30 mg lysine were dissolved in 20 mL ethanol 55% with magnetic stirring for 10 min at room temperature. Nanoparticles were obtained by the addition of 20 mL purified water. The ethanol was removed in a rotatory evaporator under reduced pressure (Büchi Rotavapor R-144; Büchi, Postfach, Switzerland) and the resulting suspension of nanoparticles was concentrated and purified by tangential flow filtration through a polysulfone membrane with a molecular weight cut off (MWCO) of 500 kDa (Spectrumlabs, California, USA) in order to remove the excess of "free" reagents that were not part of the nanoparticles (e.g., zein, PEG and lysine). Finally, 2 mL of a mannitol aqueous solution (200 mg/mL) was added to the suspension of nanoparticles and the mixture was dried in a Büchi Mini Spray Dryer B-290 apparatus (Büchi Labortechnik AG, Switzerland) under the following experimental conditions: (i) inlet temperature, 90 °C; (ii) outlet temperature, 45–50 °C; (iii) air pressure, 4–6 bar; (iv) pumping rate, 5 mL/min; (v) aspirator, 80%; and (vi) airflow, 400–500 L/h.

2.2.2. Preparation of PEG-coated nanoparticles

The coating of nanoparticles with PEG was performed by simple incubation between the just formed nanoparticles (before the purification step) and PEG 35,000 at different PEG-to-zein ratios. For this purpose, a stock solution of PEG 35,000 was prepared by dissolving the polymer in water to a final concentration of 100 mg/mL. Then, different volumes of this stock solution were added to the suspension of fresh nanoparticles. The mixture was maintained under magnetic agitation for 30 min at room temperature. After this time, nanoparticles were concentrated and purified by tangential filtration and dried as described above.

2.2.3. Preparation of fluorescently labelled nanoparticles

Nanoparticles were fluorescently labelled by the encapsulation of Lumogen® F Red 305. For this purpose, 2.6 mL of a Lumogen® red solution (concentration of 0.4 mg/mL) in ethanol was added to the solution of zein and lysine, prior to the formation of the nanoparticles. Then, nanoparticles were formed and dried as described above.

2.3. Physico-chemical characterization of nanoparticles

2.3.1. Size, polydispersity index and zeta potential

Particle size and polydispersity index (PDI) were measured after dispersion in ultrapure water, at 25 °C, by dynamic light scattering (DLS) (angle of 90°). Zeta-potential was determined by electrophoretic laser Doppler anemometry after the dispersion of nanoparticles in purified water. All of these measurements were carried out in a Zetasizer analyzer system (Brookhaven Instruments Corporation, Holtsville, USA).

2.3.2. Morphology analysis

The shape and surface morphology of the dried nanoparticles were examined by scanning electron microscopy (SEM) and transmission electron microscopy (TEM). For SEM, 1.5 mg of nanoparticles were dispersed in 1 mL deionized water and centrifuged at 9500*g* for 5 min in order to remove the mannitol. Then, the obtained pellet was redispersed in 1 mL water, mounted on SEM grids, dried and coated with a gold layer using a Quorum Technologies Q150R S sputter-coated (Ontario, Canada) and analyzed using a ZEISS Sigma 500 VP FE-SEM apparatus. For TEM, a drop of a suspension of nanoparticles was placed over a Holey Carbon film on Cu 300 mesh + thick C + SH grid (EM Resolutions, Sheffield, UK). The grid with the nanoparticle's suspension was allowed to dry and, then, images were taken using a Tecnai F30 microscope (Thermo Fischer Scientific, Oregon, USA).

2.3.3. Fourier transform infrared resonance (FTIR) analysis

The analysis of the nanoparticle's surface was carried out by infrared spectroscopy (FTIR), using a Fourier transform spectrophotometer IR Affinity-1S (Shimadzu, Japan) coupled to a Specac Golden Gate ATR. The samples analyzed were placed directly on the diamond and the spectra were collected in the mode reflectance under the following conditions: wavenumber from 600 to 4000 cm^{-1} at 2 cm^{-1} of resolution and 50 scans per spectrum. Spectra were analyzed employing the Labsolution IR software.

2.3.4. Amount of protein transformed into nanoparticles and total process yield

The amount of zein forming nanoparticles was estimated by the quantification of the protein in the eluents obtained during the purification/concentration step by UV–vis molecular absorption spectroscopy at 300 nm wavelength, using a PowerWave XS Microplate reader (Bio-Tek Instruments, Inc; Vermont, USA). The standard curve was prepared by dissolving increasing concentrations of pure zein in ethanol 70%. The amount of protein forming nanoparticles in the formulation was estimated as the ratio between the amount of the protein quantified in the elute and the total amount of protein used for the preparation of

nanoparticles, and, expressed as a percentage.

Finally, the yield of the whole preparative process of nanoparticles was calculated by gravimetry (Arbós et al., 2002).

2.3.5. Surface hydrophobicity evaluation

The surface hydrophobicity of the different nanoparticles was evaluated by the Rose Bengal method (Doktorovova et al., 2012). Briefly, 500 μL of nanoparticle suspensions (from 0.03 to 3 mg/mL) were mixed with 1 mL of a Rose Bengal aqueous solution (100 μg/mL). All samples were incubated under constant shaking at 1500 rpm, for 30 min at 25 °C (Labnet VorTemp 56 EVC, Labnet International, Inc. New Jersey, USA). Afterwards, the samples were centrifuged at 13,500*g* for 30 min (centrifuge MIKRO 220, Hettich, Germany) to remove the nanoparticles. The amount of Rose Bengal in the supernatants (Rose Bengal unbound) was calculated by measuring the absorbance at 548 nm, using a PowerWave XS Microplate reader (BioTek Instruments, Inc., Vermont, USA).

For calculations, the total surface area (TSA) of nanoparticles (calculated using Eq. (1)) was determined by assuming that the nanoparticles were spherical in shape and monodisperse, with a diameter equal to the mean size determined by DLS.

$$TSA = (SA_{NP}) \times (NT_{NP}) \quad (1)$$

where SA_{NP} is the surface of one individual nanoparticle ($4\pi r^2$), and NT_{NP} is the total number of nanoparticles in each dilution, calculated using the Eq. (2):

$$NT_{NP} = m_{NP}/(\rho zein \times V_{NP}) \quad (2)$$

where m_{NP} is the weight of the nanoparticles in each dilution, ρzein is the density of zein (1.41 g/mL calculated by pycnometry) and V_{NP} is the volume ($4/3\pi r^3$) of an individual nanoparticle.

On the other hand, the partitioning quotient (PQ) was calculated as the quotient between the amount of the Rose bengal bound and unbound. The slope of the line of the chart represents the hydrophobicity of the formulation. The higher the slope, the higher the hydrophobicity.

2.4. Ex vivo mucus diffusion studies in porcine intestinal mucus

2.4.1. Collection and preparation of porcine mucus

The native porcine mucus was harvested from small intestine. The intestines were collected from a slaughterhouse and kept in ice-cold PBS (for a maximum period of 2 h) prior to the mucus collection. Intestine was cut into small portions that were opened to expose the lumen. Then, the exposed lumen was cleaned with PBS and the mucus collected using a spatula. The scraping was very gently in order not to drag epithelial tissue. A single pool of mucus was obtained, which was then distributed in 0.5 g-aliquots in microtubes that were stored at −80 °C until the moment of use.

2.4.2. Evaluation of the diffusion of nanoparticles in mucus by multiple Particle tracking (MPT)

The diffusion of the nanoparticles through pig intestinal mucus, as an in vitro measurement of their mucus-permeating properties, was assessed by the Multiple Particle Tracking (MPT) technique (Abdulkarim et al., 2015; Rohrer et al., 2016).

MPT involves video capturing and post-acquisition analysis for the individual movement of hundreds of fluorescently labelled particles within a mucus matrix (Grießinger et al., 2015). 25 μL of a suspension of fluorescently labelled nanoparticles (4 mg/mL in water) were inoculated into approximately 0.5 g of mucus aliquots. Each sample was incubated under agitation for 2 h at 37 °C in order to ensure effective particle distribution before the video recording. Two-dimensional videos were captured in a Leica DM IRB wide-field epifluorescence microscope (×63 magnification) using a high-speed camera (Allied Vision Technologies, UK) and capturing 30 frames/second; 10 s videos (i.e. complete video comprised 300 frames). At least 100 individual trajectories were tracked and analyzed from each mucus sample. Examples of videos, for bare (NP) and PEG-coated nanoparticles (NP-PEG50), are included in the Supplementary Material section. The MPT of each formulation was carried out in triplicates, leading to a minimum of 300 individual trajectories assessed. Videos were analyzed using Fiji (Image J). Only trajectories longer than 30 frames were considered, in order to ensure a continuous presence of the individual nanoparticles in the X-Y plane. The trajectory of each nanoparticle was then converted into numeric pixel data and, finally, into metric distances (based on the recording settings). The displacement of each nanoparticle overtime was expressed as the squared displacement (SD), and the mean square displacement (MSD) was calculated as the geometric mean of that nanoparticle's squared displacement along its entire trajectory. MSD was determined as follows:

$$MSD = (X\Delta t)^2 + (Y\Delta t)^2 \quad (3)$$

For each nanoparticle formulation studied, the "ensemble mean square displacement" (<MSD >) was determined for each of the replicates by calculating the geometric mean of 100 individual trajectories. Then, the effective diffusion coefficient (D_{eff}) of each formulation was calculated by:

$$D_{eff} = < MSD > /(4 \times \Delta t) \quad (4)$$

Where 4 is a constant relating to the 2-dimensional mode of video capturing and Δt is the selected time interval.

In parallel, the diffusion of the nanoparticles in water (D°) was calculated by the Stokes–Einstein equation at 37 °C:

$$D^\circ = kT6\pi\eta r \quad (5)$$

In which *k* is the Boltzmann constant, *T* is absolute temperature, η is water viscosity and *r* is the mean radius of nanoparticles.

Finally, the diffusion of all the formulations was expressed as the ratio (%) between their D_{eff} and their D° (diffusions in mucus and in water, respectively). This ratio provides a measure of the relative diffusion of the nanoparticles in mucus when considering their Brownian motion in water. For the graphical representation and for each formulation, these ratios were normalized to the ratio obtained for bare nanoparticles.

2.5. In vivo biodistribution evaluation of nanoparticles in healthy rats

The biodistribution of the nanoparticles in the gastrointestinal tract of male Wistar rats (weight 180–220 g; Envigo, Indianapolis, USA) was visualized by fluorescence microscopy (Inchaurraga et al., 2015). Animals were housed under controlled temperature (23 ± 2 °C) with 12-h light/dark cycles and with free access to normal chow and water. All experiments were performed after a minimum acclimation period of 7 days. Prior to any procedure, animals were fasted overnight. During the procedures, animals were kept fasted but with free access to water. All the procedures were performed following a protocol previously approved by the "Ethical and Biosafety Committee for Research on Animals" at the University of Navarra in line with the European legislation on animal experiments (protocol 045-18). For the study, 10 mg of fluorescently labelled nanoparticles dispersed in 1 mL purified water were orally administered to fasted animals. Two hours post-administration, animals were sacrificed by cervical dislocation and the guts were removed. Tissue portions of 1 cm were collected, washed with PBS, and frozen at −80 °C after inclusion in the tissue proceeding medium O.C.T.™. Each portion was then cut into 5 μm sections on a cryostat and attached to glass slides. Finally, the slices were fixed with formaldehyde and stained with DAPI for 15 min. before the cover assembly. The presence of fluorescently loaded zein nanoparticles in the intestinal mucosa and the cell nuclei of intestinal cells, dyed with DAPI, were visualized in a fluorescence microscope (Axioimager M1, Zeiss; Oberkochen, Germany) with a coupled camera (Axiocam ICc3, Zeiss) and fluorescent source (HBO 100, Zeiss). The images were captured with

the software ZEN (Zeiss). The post-acquisition processing of the images was carried out with the software Fiji (Image J).

As control, an aqueous suspension of Lumogen® F Red 305 was administered.

2.6. Statistical analysis

The means and standard errors were calculated for every data set. All the group comparisons and statistical analyses were performed using a one-way ANOVA test followed by a Tukey-Kramer multicomparison test. In all cases, $p < 0.05$ was considered as a statistically significant difference. All calculations were performed using Graphpad Prism v6 (California, USA) and the curves were plotted with the Origin 8 software from Origin Lab (Massachusetts, USA).

3. Results

3.1. Nanoparticles characterization

The main physico-chemical characteristics of bare nanoparticles and nanoparticles coated at different PEG-to-zein ratios are shown in Table 1. The coating with PEG did not significantly modify the mean size of the resulting nanoparticles, with a typical diameter close to 200 nm and a polydispersity index (PDI) lower than 0.15. The morphological analysis by scanning electron microscopy (SEM) showed that all the formulations consisted of a homogeneous population of spherical-shaped nanoparticles (Fig. 1), with no apparent differences between bare and PEG-coated nanoparticles. Likely, the size values obtained by this technique were similar to those obtained by dynamic light scattering. By TEM (Fig. 1C), the presence of a less dense substance (corresponding to the PEG-coating) on the surface of zein nanoparticles was observed. Moreover, the coating with PEG slightly decreased the negative zeta potential of the resulting nanoparticles. In addition, the amount of zein transformed into nanoparticles was, in all cases, close to 80%. This value was not affected by the coating with PEG. Finally, the total preparative process yield (after the drying step) was calculated to be around 60%, without differences between formulations.

Fig. 2 shows the FTIR spectra of the different nanoparticles and the raw materials employed in their preparation. The FTIR analysis demonstrated the presence of PEG in the nanoparticles after their formulation and drying. For all the formulations and for the free zein, two characteristic stretching vibration bands of amide I and amide II groups (at 1637 and 1521 cm^{-1}, respectively) were observed. The amide I band is associated with the C = O stretching and the amide II absorption peak is associated to C-N and N-H stretching vibrations. Regarding the FTIR spectrum of PEG, among others, the following typical signals were found: the vibration of CH_2 groups (1465 cm^{-1}), the stretching vibration of C-O-C (1143 cm^{-1}) or the C-O vibration of the OH end group of PEG (1093 cm^{-1}). The spectra of nanoparticles showed a displacement in the amide I stretching vibration band, which may be consequence of a conformational change when the nanoparticles are formed. Furthermore, in the spectra of PEG-coated nanoparticles obtained at a PEG-to-zein ratio higher than 0.05, some of the polymer vibration bands were clearly detected (1465, 1143 and 1058 cm^{-1}); confirming the presence of PEG on the surface of the nanoparticles. In addition, it is worth noting the shift of the vibration band corresponding to the alcoholic group of PEG (1093–1101 cm^{-1}) as well as that associated to the amide II of zein. This finding would indicate a possible interaction between the protein and the polymer through the formation of hydrogen bonds. Finally, absorption peaks corresponding to lysine (1577, 1408, 1358 cm^{-1}) were also detected in all the nanoparticle formulations.

Fig. 3 shows the surface hydrophobicity of nanoparticles, calculated by means of the Rose Bengal test, as a function of the PEG-to-zein ratio employed in the preparation of nanoparticles. The coating of nanoparticles with PEG 35,000 significantly reduced the surface hydrophobicity, and this effect was found to be dependent on the amount of PEG employed during the coating process. Thus, the surface hydrophobicity of NP-PEG5 was calculated to be about 60% of the value determined for bare nanoparticles, whereas for NP-PEG75, the hydrophobicity was 4-times lower than for NP.

3.2. Ex vivo mucus diffusion studies in porcine intestinal mucus

Table 2 summarizes the main parameters defining the diffusivity of the nanoparticles and Fig. 4 shows the capability of the different formulations to diffuse through pig intestinal mucus. Again, the coating of zein nanoparticles with PEG 35,000 significantly increased their ability to move and diffuse within mucus. Thus, for nanoparticles prepared at a PEG-to-zein ratio similar or higher than 0.25, their diffusivity in pig intestinal mucus was about 8-times higher than for bare nanoparticles.

3.3. In vivo evaluation of the mucus-permeating properties of nanoparticles in healthy rats

Fig. 5 shows fluorescence micrographs of duodenum slices obtained 2 h post-administration of different Lumogen-loaded formulations to animals. On the one hand, both bare and PEG-coated nanoparticles at a PEG-to-zein ratio of 0.05 displayed a localization that seemed to be restricted to the mucus layer covering the epithelium, without presence between intestinal villi. On the other hand, PEG-coated nanoparticles prepared at a PEG-to-zein ratio higher than 0.05 were clearly seen in close contact with the intestinal epithelium, occupying the inter-villi spaces and, even reaching the intestinal crypts. Afterwards, the biodistribution of mucoadhesive and mucus-permeating formulations (NP and NP-PEG50, respectively) along the gastrointestinal tract were evaluated (Fig. 6). In the small intestine (Fig. 6C–F), mucus-permeating nanocarriers were able to diffuse through the protective mucus layer and reach the epithelium surface. Finally, in the cecum of animals, only fluorescence associated to NP-PEG50 was visualized, suggesting the capability of these nanoparticles to reach this region of the gut 2 h post-administration.

4. Discussion

This study aimed to develop suitable oral nanocarriers with mucus-permeating properties based on GRAS material and produced by a simple, cheap and reliable procedure. For that purpose, zein (GRAS protein) was chosen to generate the nanoparticles. These nanoparticles have shown (as other nanocarriers based on proteins) an interesting

Table 1
Physico-chemical characteristics of bare (NP) and PEG-coated nanoparticles at different PEG-to-zein ratios (5%, 25%, 50% and 75%; w/w). Data expressed as mean ± SD, $n \geq 3$.

	Size (nm)	PDI	Zeta potential (mv)	Amount of protein (%)	Total process yield (%)
NP	200 ± 15	0.04 ± 0.03	−54 ± 4	82.8 ± 1.7	61.3 ± 5.6
NP-PEG5	203 ± 8	0.05 ± 0.02	−51 ± 3	80.8 ± 1.6	58.5 ± 1.8
NP-PEG25	202 ± 9	0.06 ± 0.02	−49 ± 2	77.4 ± 3.7	57.9 ± 3.9
NP-PEG50	201 ± 14	0.08 ± 0.01	−50 ± 2	81.5 ± 2.4	61.6 ± 9.8
NP-PEG75	213 ± 18	0.07 ± 0.02	−51 ± 2	82.8 ± 1.3	60.5 ± 1.8

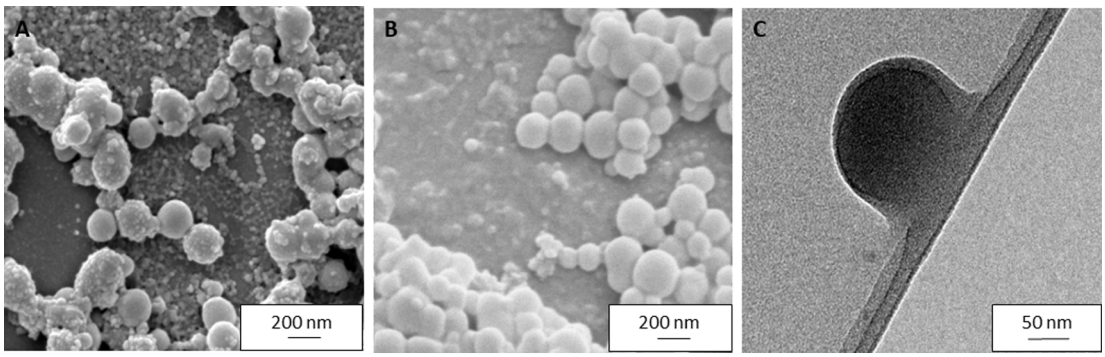

Fig. 1. Microphotographs of bare nanoparticles (NP) and PEG-coated nanoparticles (NP-PEG50). A: NP obtained by SEM; B: NP-PEG50 obtained by SEM; C: NP-PEG50 obtained by TEM.

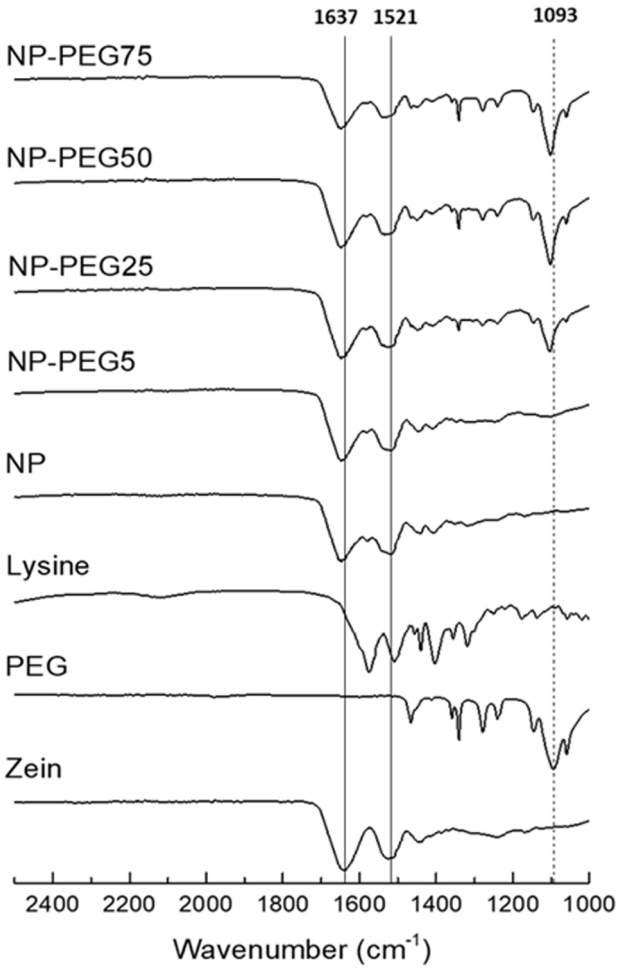

Fig. 2. FTIR spectra of zein, PEG 35,000, lysine, bare zein nanoparticles and PEG-coated zein nanoparticles. Straight lines correspond to 1637 and 1521 cm^{-1} stretching vibration bands. Dashed line corresponds to 1093 cm^{-1} band.

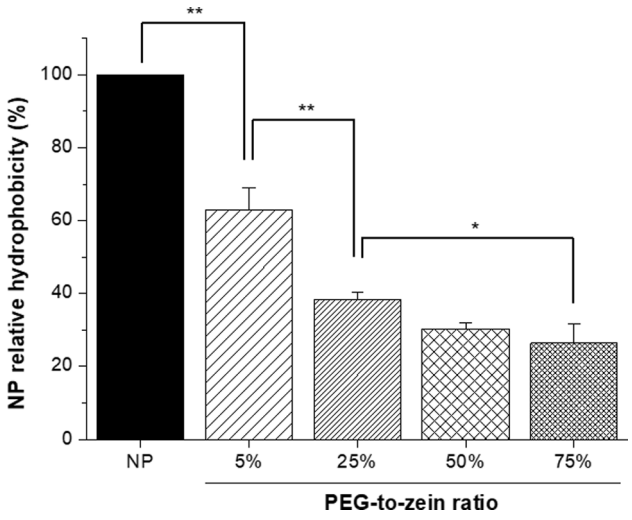

Fig. 3. Surface hydrophobicity of the different formulations. Values are normalized to the hydrophobicity of bare nanoparticles (NP). PEG-to-zein ratio is expressed in percentage. Data expressed as mean ± SD ($n = 3$). *: $p < 0.05$; **: $p < 0.01$.

Table 2
Diffusion behavior of the different formulations tested. $< D_{eff} >$: diffusion coefficient in mucus; D°: theoretical diffusion coefficient in water; $< D_{eff} > / D^{\circ}$: quotient between the diffusion coefficients of nanoparticles in mucus and water, respectively (expressed in percentage). Data expressed as mean ± SD, n = 3.

	<Deff> (mucus) $cm^2 \times S^{-1} \times 10^{-9}$	D° (water) $cm^2 \times S^{-1} \times 10^{-9}$	<Deff>/D° (%)
NP	0.054 ± 0.038	23.47	0.23 ± 0.11
NP-PEG5	0.169 ± 0.085	24.85	0.68 ± 0.03
NP-PEG25	0.473 ± 0.237	24.76	1.91 ± 0.07
NP-PEG50	0.447 ± 0.226	22.35	2.00 ± 0.15
NP-PEG75	0.479 ± 0.244	23.02	2.08 ± 0.15

ability to encapsulate both hydrophobic small molecules (i.e., glibenclamide (Lucio et al., 2017)) and hydrophilic biomacromolecules (e,g., insulin (Inchaurraga et al., 2020)). However, and particularly for the oral delivery of therapeutic proteins, conventional zein nanoparticles (NP) do not provide the required increase in bioavailability necessary for a clinical application. In order to minimize this problem, one alternative would be the use of zein nanoparticles with mucus-permeating properties. For this purpose, zein nanoparticles were coated with a hydrophilic polymer (PEG) at different PEG-to-zein ratios. This coating would reduce the interactions between the nanoparticle and the mucus matrix, conferring mucus-penetrating nanoparticles. The capability of PEG to confer mucus-permeating properties relies on its molecular weight and grafting density, which, in last term, will determine its conformation (Inchaurraga et al., 2015; Xu et al., 2015). In fact, PEG with MW as high as 40 kDa, if densely grafted to the surface of nanoparticles, would prevent their interactions with mucus, conferring a mucoinert surface (Maisel et al., 2016). Since the coating occurs by physical adsorption, no new chemical entities are generated during the

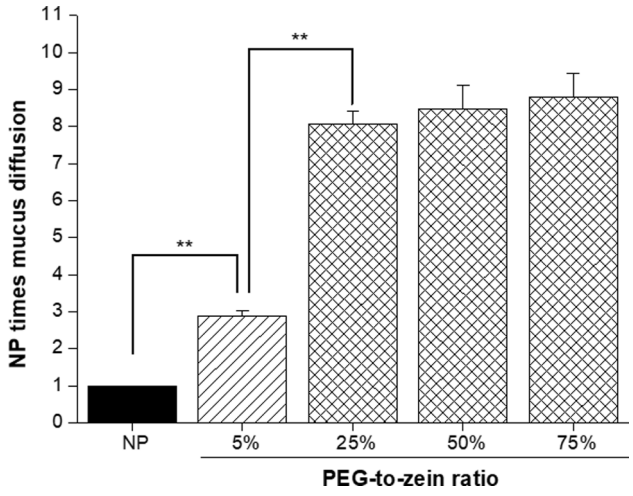

Fig. 4. Comparative of the capability of nanoparticles (bare and PEG-coated) to diffuse through pig intestinal mucus. Values are normalized to the diffusion of bare nanoparticles (NP diffusion in intestinal mucus = 1). PEG-to-zein ratio is expressed in percentage. Data expressed as mean ± SD ($n = 3$). **: $p < 0.01$.

formulation of PEG-coated zein nanoparticles. Thus, this method leads to the formation of mucus-permeating nanoparticles composed only by GRAS materials, what would facilitate a faster clinical development (Ensign et al., 2012; Yu et al., 2012).

All the formulations were prepared by a desolvation method and the coating of the just formed nanoparticles with PEG was carried out by simple incubation. During the preparative process of nanoparticles, no type of organic solvent (apart from ethanol) was used. In addition, during the evaporation step, the ethanol used can be recovered and, later, reused. All of the resulting nanoparticles displayed a mean size of about 200 nm, independently of the PEG-to-zein ratio, and a negative zeta potential. Likely, under the experimental conditions tested, the amount of protein transformed into nanoparticles was high (about 80%), whereas the total yield of the process was calculated to be close to 60%. This last result may be considered low but it is in line with previous results using similar lab-scale Spray-dryer apparatus and might be improved during scale-up (Li et al., 2010; Ngan et al., 2014). In fact, it is well known that, in the particular case of Spray-drying, the yield of the process increases by increasing the size of batches (Draheim et al., 2015). The scanning electron microscopy confirmed the size, shape, and the homogeneity of the formulations measured by DLS. Nanoparticles were round-shaped with a smooth surface (Fig. 1A and 1B). Interestingly, the incubation of nanoparticles with PEG produced a

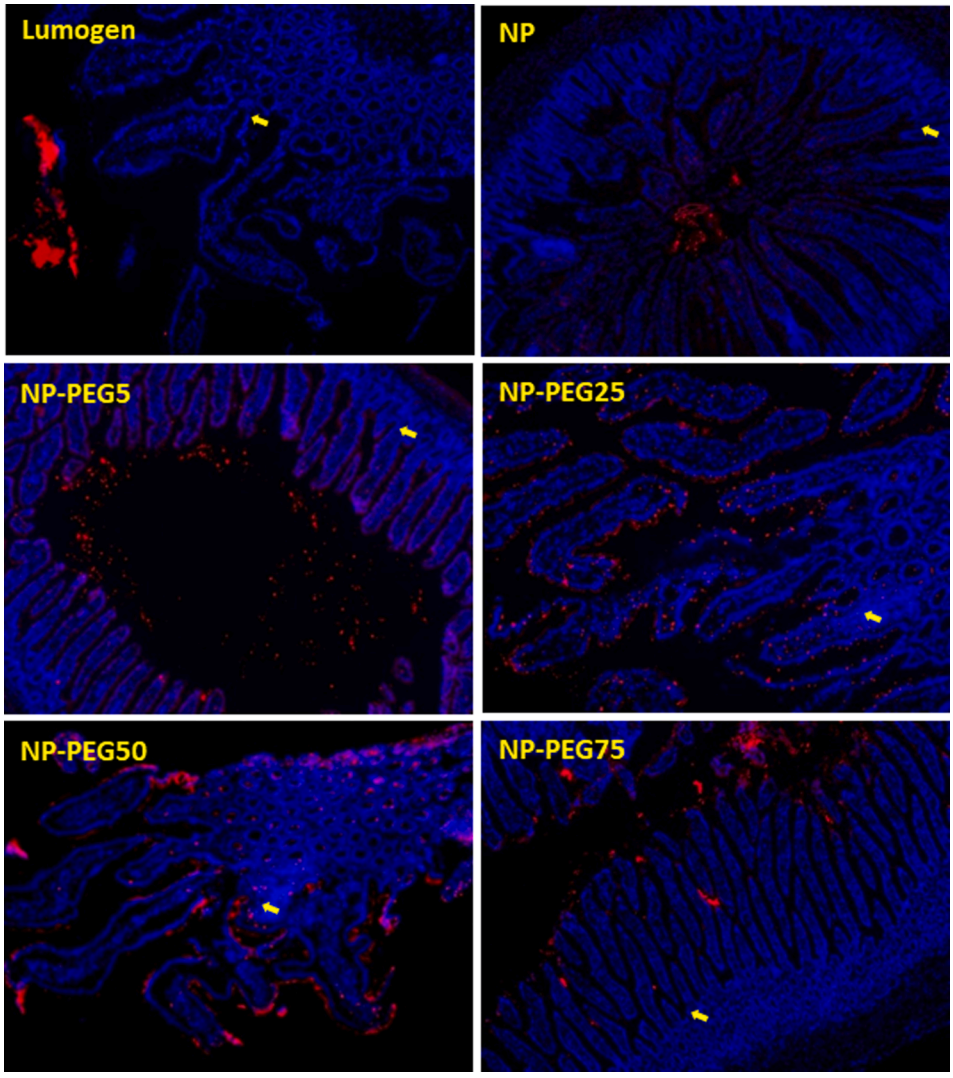

Fig. 5. Fluorescence microscopic visualization of a lumogen aqueous suspension, bare nanoparticles (NP), and PEG-coated nanoparticles in sections of rat duodenums 2 h after oral administration. Yellow arrows point to intestinal crypts. Nuclei of cells, stained with DAPI, are seen in blue.

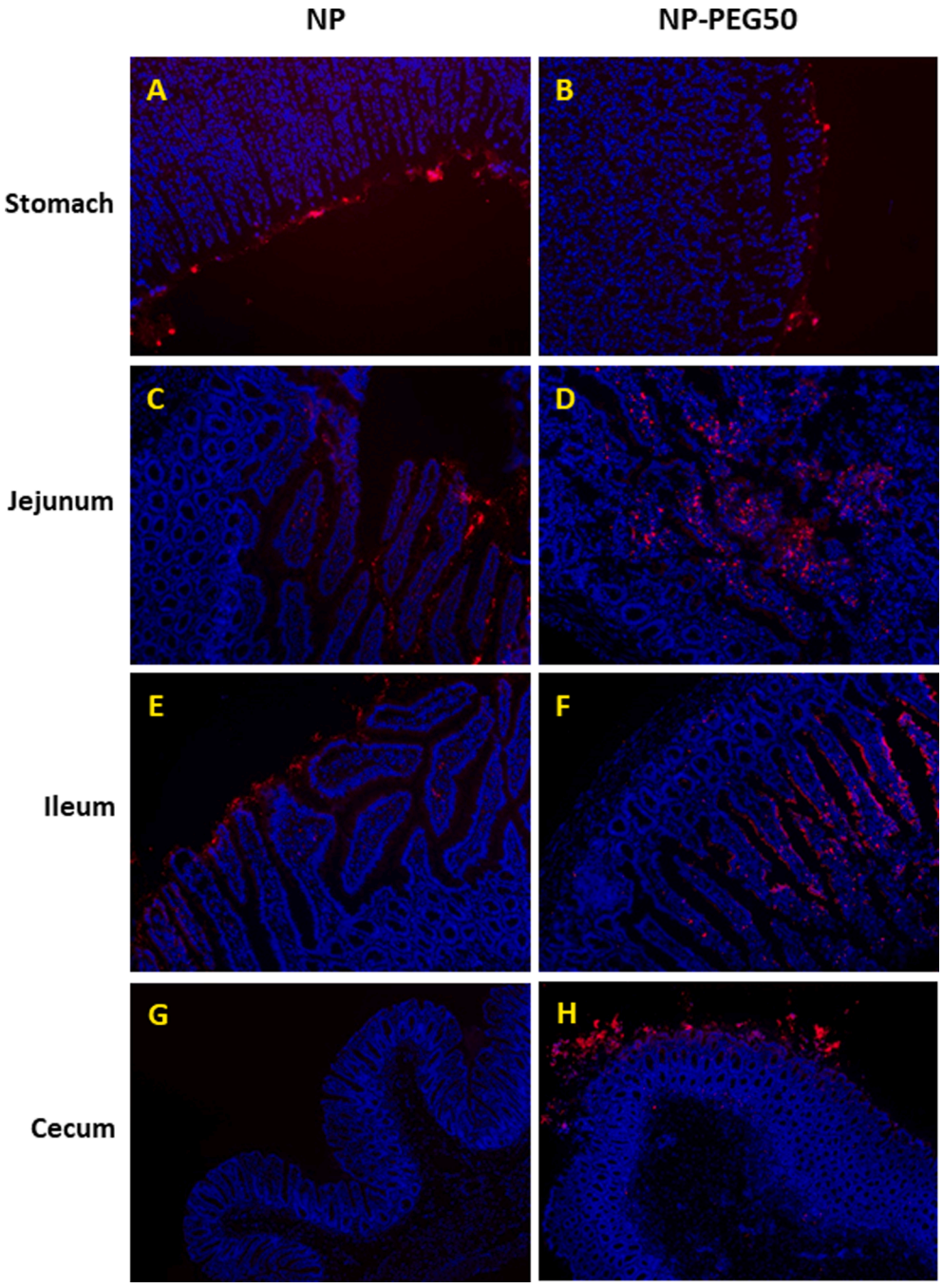

Fig. 6. Fluorescence microscopic visualization of bare nanoparticles (NP) and nanoparticles coated with PEG at a PEG-to-zein ratio of 0.5 (NP-PEG50) in slices of the different portions of the gastrointestinal tract of animals, 2 h post-administration. A and B show slices from the stomachs of animals, C and D from jejunums, E and F from ileums, and G and H from cecums. Nuclei of cells, stained with DAPI, are seen in blue. (For interpretation of the references to colour in this figure legend, the reader is referred to the web version of this article.)

homogeneous layer around the surface of nanoparticles of about 10 nm (Fig. 1C). This finding was corroborated by FTIR analysis (Fig. 2) which not only showed the presence of the most characteristic PEG bands but also that the size of these signals increased by increasing the PEG-to-zein ratio. Considering all these data, it is possible to hypothesize an intermolecular interaction between PEG and zein. This interaction could be driven by a combination of hydrogen bonds (as predicted by the FTIR results) with other weak PEG-protein interactions (e.g., Van der Waals forces) (Wu et al., 2014).

The hydrophobic surface of zein nanoparticles was significantly reduced by their coating with PEG (Fig. 3). This increase of the hydrophilicity of nanoparticles was associated with an important increase of their mobility in pig intestinal mucus (Fig. 4), in line with previous results demonstrating that the PEGylation of polymer nanoparticles produced important improvements in their diffusive properties in mucus (Laffleur et al., 2014; Xu et al., 2015). In addition, in our case, a good correlation between hydrophobicity and mucus diffusivity was obtained ($R^2 = 0.93$; Fig. 7).

The biodistribution assays carried out in rats revealed that, 2 h post-administration of fluorescently labelled nanoparticles, bare zein nanoparticles and NP-PEG5 were found mainly entangled into the mucus layer of the duodenum, far away from the absorptive epithelium (Fig. 5). Likely, this finding agreed well with a higher hydrophobicity and lower diffusivity in pig intestinal mucus (as measured by MPT). On the contrary, under the same conditions, nanoparticles prepared at a PEG-to-zein ratio similar or higher than 0.25 (with lower hydrophobicity and higher diffusivity in mucus than bare nanoparticles) were localized in close contact with the epithelium (Fig. 5). In a similar way, NP-PEG50 were found in the cecum 2 h post-administration, while bare nanoparticles did not reach this portion of the gastrointestinal tract (Fig. 6H

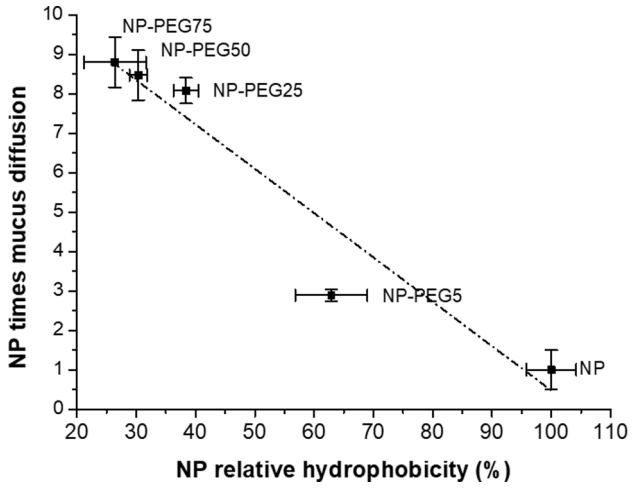

Fig. 7. Correlation between the capability of PEG-coated zein nanoparticles (prepared at different PEG-to-zein ratios) to diffuse in pig intestinal mucus and their surface hydrophobicity. Both parameters are normalized to the values of bare nanoparticles. Data expressed as mean ± SD (n = 3).

and G, respectively). This, once again, reinforces the mucus-permeating properties of the PEG coating. The fact that NP-PEG50 reached the cecum might be because their increased diffusivity is applied not only for a transversal flow through the mucus gel, what allows them to reach the epithelium, but also for longitudinal flowing all along the gastrointestinal tract.

In summary, PEG-coated zein nanoparticles may be prepared by a desolvation procedure, subsequent purification by tangential flow filtration, and drying in a spray-drier. The preparative process is simple and reproducible, without employing reactive reagents. The PEG layer on the surface of zein nanoparticles conferred a hydrophilic corona and a superior capability to diffuse in pig intestinal mucus than bare nanoparticles. *In vivo*, PEG-coated nanoparticles showed mucus-permeating properties with an important ability to reach the gut epithelium and appeared to move more rapidly along the gut, reaching the cecum two-hours post-administration.

Declaration of Competing Interest

The authors declare that they have no known competing financial interests or personal relationships that could have appeared to influence the work reported in this paper.

Acknowledgements

The first author acknowledges to the ADA-Universidad de Navarra for a Ph. D. scholarship.

Appendix A. Supplementary material

Supplementary data to this article can be found online at https://doi.org/10.1016/j.ijpharm.2021.120287.

References

Abdulkarim, M., Agulló, N., Cattoz, B., Griffiths, P., Bernkop-Schnürch, A., Borros, S.G., Gumbleton, M., 2015. Nanoparticle diffusion within intestinal mucus: Three-dimensional response analysis dissecting the impact of particle surface charge, size and heterogeneity across polyelectrolyte, pegylated and viral particles. Eur. J. Pharm. Biopharm. 97, 230–238. https://doi.org/10.1016/J.EJPB.2015.01.023.

Arbós, P., Arangoa, M.A., Campanero, M.A., Irache, J.M., 2002. Quantification of the bioadhesive properties of protein-coated PVM/MA nanoparticles. Int. J. Pharm. 242, 129–136. https://doi.org/10.1016/S0378-5173(02)00182-5.

Bhardwaj, V., Kaushik, A., Khatib, Z.M., Nair, M., McGoron, A.J., 2019. Recalcitrant issues and new frontiers in nano-pharmacology. Front. Pharmacol. 10, 1369. https://doi.org/10.3389/fphar.2019.01369.

Bremer-Hoffmann, S., Halamoda-Kenzaoui, B., Borgos, S.E., 2018. Identification of regulatory needs for nanomedicines. J. Interdiscip. Nanomed. 3, 4–15. https://doi.org/10.1002/jin2.34.

Cicha, I., Chauvierre, C., Texier, I., Cabella, C., Metselaar, J.M., Szebeni, J., Dézsi, L., Alexiou, C., Rouzet, F., Storm, G., Stroes, E., Bruce, D., MacRitchie, N., Maffia, P., Letourneur, D., 2018. From design to the clinic: Practical guidelines for translating cardiovascular nanomedicine. Cardiovasc. Res. 114, 1714–1727. https://doi.org/10.1093/cvr/cvy219.

ClinicalTrials.gov [WWW Document], 2021. URL https://www.clinicaltrials.gov/ct2/result (accessed 1.14.21).

D'souza, A.A., Shegokar, R., 2016. Polyethylene glycol (PEG): a versatile polymer for pharmaceutical applications. Exp. Opin. Drug Deliv. 13, 1257–1275. https://doi.org/10.1080/17425247.2016.1182485.

Doktorovova, S., Shegokar, R., Martins-Lopes, P., Silva, A.M., Lopes, C.M., Müller, R.H., Souto, E.B., 2012. Modified Rose Bengal assay for surface hydrophobicity evaluation of cationic solid lipid nanoparticles (cSLN). Eur. J. Pharm. Sci. 45, 606–612. https://doi.org/10.1016/J.EJPS.2011.12.016.

Draheim, C., De Crécy, F., Hansen, S., Collnot, E.M., Lehr, C.M., 2015. A design of experiment study of nanoprecipitation and nano spray drying as processes to prepare plga nano-and microparticles with defined sizes and size distributions. Pharm. Res. 32, 2609–2624. https://doi.org/10.1007/s11095-015-1647-9.

Ensign, L.M., Schneider, C., Suk, J.S., Cone, R., Hanes, J., 2012. Mucus penetrating nanoparticles: Biophysical tool and method of drug and gene delivery. Adv. Mater. 24, 3887–3894. https://doi.org/10.1002/adma.201201800.

Gaspani, S., Milani, B., 2013. Access to liposomal generic formulations: beyond Am Bisome and Doxil/Caelyx. Generics Biosimilars Initiat. J. 2, 60–63.

Grießinger, J., Dünnhaupt, S., Cattoz, B., Griffiths, P., Oh, S., Gómez, S.B. i, Wilcox, M., Pearson, J., Gumbleton, M., Abdulkarim, M., Pereira de Sousa, I., Bernkop-Schnürch, A., 2015. Methods to determine the interactions of micro- and nanoparticles with mucus. Eur. J. Pharm. Biopharm. 96, 464–476. https://doi.org/10.1016/J.EJPB.2015.01.005.

Gurunathan, S., Kang, M.H., Qasim, M., Kim, J.H., 2018. Nanoparticle-mediated combination therapy: Two-in-one approach for cancer. Int. J. Mol. Sci. 19, 3264. https://doi.org/10.3390/ijms19103264.

Hua, S., de Matos, M.B.C., Metselaar, J.M., Storm, G., 2018. Current trends and challenges in the clinical translation of nanoparticulate nanomedicines: Pathways for translational development and commercialization. Front. Pharmacol. 9, 790. https://doi.org/10.3389/fphar.2018.00790.

Inchaurraga, L., Martín-Arbella, N., Zabaleta, V., Quincoces, G., Peñuelas, I., Irache, J.M., 2015. In vivo study of the mucus-permeating properties of PEG-coated nanoparticles following oral administration. Eur. J. Pharm. Biopharm. 97, 280–289. https://doi.org/10.1016/J.EJPB.2014.12.021.

Inchaurraga, L., Martínez-López, A.L., Martin-Arbella, N., Irache, J.M., 2020. Zein-based nanoparticles for the oral delivery of insulin. Drug Deliv. Transl. Res. 10, 1601–1611. https://doi.org/10.1007/s13346-020-00796-3.

Irache, J.M., Esparza, I., Gamazo, C., Agüeros, M., Espuelas, S., 2011. Nanomedicine: Novel approaches in human and veterinary therapeutics. Vet. Parasitol. 180, 47–71. https://doi.org/10.1016/J.VETPAR.2011.05.028.

Irache, J.M., González-Navarro, C.J., 2017. Zein nanoparticles as vehicles for oral delivery purposes. Nanomedicine 12, 1209–1211. https://doi.org/10.2217/nnm-2017-0075.

Laffleur, F., Hintzen, F., Shahnaz, G., Rahmat, D., Leithner, K., Bernkop-Schnürch, A., 2014. Development and in vitro evaluation of slippery nanoparticles for enhanced diffusion through native mucus. Nanomedicine 9, 387–396. https://doi.org/10.2217/nnm.13.26.

Li, X., Anton, N., Arpagaus, C., Belleteix, F., Vandamme, T.F., 2010. Nanoparticles by spray drying using innovative new technology: The Büchi Nano Spray Dryer B-90. J. Control. Release 147, 304–310. https://doi.org/10.1016/j.jconrel.2010.07.113.

Lucio, D., Martínez-Ohárriz, M.C., Jaras, G., Aranaz, P., González-Navarro, C.J., Radulescu, A., Irache, J.M., 2017. Optimization and evaluation of zein nanoparticles to improve the oral delivery of glibenclamide. In vivo study using *C. elegans*. Eur. J. Pharm. Biopharm. 121, 104–112. https://doi.org/10.1016/j.ejpb.2017.09.018.

Ma, P., Mumper, R.J., 2013. Paclitaxel nano-delivery systems: A comprehensive review. J. Nanomed. Nanotechnol. 4, 6. https://doi.org/10.4172/2157-7439.1000164.

Maisel, K., Reddy, M., Xu, Q., Chattopadhyay, S., Cone, R., Ensign, L.M., Hanes, J., 2016. Nanoparticles coated with high molecular weight PEG penetrate mucus and provide uniform vaginal and colorectal distribution in vivo. Nanomedicine 11, 1337–1343. https://doi.org/10.2217/nnm-2016-0047.

Martins, J.P., das Neves, J., de la Fuente, M., Celia, C., Florindo, H., Günday-Türeli, N., Popat, A., Santos, J.L., Sousa, F., Schmid, R., Wolfram, J., Sarmento, B., Santos, H.A., 2020. The solid progress of nanomedicine. Drug Deliv. Transl. Res. 10, 726–729. https://doi.org/10.1007/s13346-020-00743-2.

Netsomboon, K., Bernkop-Schnürch, A., 2016. Mucoadhesive vs. mucopenetrating particulate drug delivery. Eur. J. Pharm. Biopharm. 98, 76–89. https://doi.org/10.1016/J.EJPB.2015.11.003.

Ngan, L.T.K., Wang, S.L., Hiep, I.M., Luong, P.M., Vui, N.T., Signinh, T.M. Crossed D, Dzung, N.A., 2014. Preparation of chitosan nanoparticles by spray drying, and their antibacterial activity. Res. Chem. Intermed. 40, 2165–2175. https://doi.org/10.1007/s11164-014-1594-9.

Penalva, R., Esparza, I., Larraneta, E., González-Navarro, C.J., Gamazo, C., Irache, J.M., 2015. Zein-Based Nanoparticles Improve the Oral Bioavailability of Resveratrol and Its Anti-inflammatory Effects in a Mouse Model of Endotoxic Shock. J. Agric. Food Chem. 63, 5603–5611. https://doi.org/10.1021/jf505694e.

Pison, U., Welte, T., Giersig, M., Groneberg, D.A., 2006. Nanomedicine for respiratory diseases. Eur. J. Pharmacol. 533, 341–350. https://doi.org/10.1016/j.ejphar.2005.12.068.

Rohrer, J., Partenhauser, A., Hauptstein, S., Gallati, C.M., Matuszczak, B., Abdulkarim, M., Gumbleton, M., Bernkop-Schnürch, A., 2016. Mucus permeating thiolated self-emulsifying drug delivery systems. Eur. J. Pharm. Biopharm. 98, 90–97. https://doi.org/10.1016/j.ejpb.2015.11.004.

Singh, R., Nalwa, H.S., 2011. Medical applications of nanoparticles in biological imaging, cell labeling, antimicrobial agents, and anticancer nanodrugs. J. Biomed. Nanotechnol. 7, 489–503. https://doi.org/10.1166/jbn.2011.1324.

Vinogradov, S., Wei, X., 2012. Cancer stem cells and drug resistance: the potential of nanomedicine. Nanomedicine 7, 597–615. https://doi.org/10.2217/nnm.12.22.

Wu, J., Zhao, C., Lin, W., Hu, R., Wang, Q., Chen, H., Li, L., Chen, S., Zheng, J., 2014. Binding characteristics between polyethylene glycol (PEG) and proteins in aqueous solution. J. Mater. Chem. B 2, 2983–2992. https://doi.org/10.1039/c4tb00253a.

Xu, Q., Ensign, L.M., Boylan, N.J., Schön, A., Gong, X., Yang, J.-C., Lamb, N.W., Cai, S., Yu, T., Freire, E., Hanes, J., 2015. Impact of Surface Polyethylene Glycol (PEG) Density on Biodegradable Nanoparticle Transport in Mucus ex Vivo and Distribution in Vivo. ACS Nano 9, 9217–9227. https://doi.org/10.1021/acsnano.5b03876.

Yu, T., Wang, Y.Y., Yang, M., Schneider, C., Zhong, W., Pulicare, S., Choi, W.J., Mert, O., Fu, J., Lai, S.K., Hanes, J., 2012. Biodegradable mucus-penetrating nanoparticles composed of diblock copolymers of polyethylene glycol and poly(lactic-co-glycolic acid). Drug Deliv. Transl. Res. 2, 124–128. https://doi.org/10.1007/s13346-011-0048-9.